AD-7/GBAR status report for the 2014 CERN SPSC

P. Dupré [1], P. Grandemange[1], D. Lunney[1], V. Manea[1], A. Badertscher[2], D. Banerjee[2], P. Crivelli[2], A. Curioni[2], A. Marchionni[2], B. Rossi[2], A. Rubbia[2], V. Nesvizhevsky[3], P-A. Hervieux[4], G. Manfredi[4], D. Brook-Roberge[5], P. Comini[5], P. Debu[5], L. Liszkay[5], B. Mansoulié[5], T. Mortensen[5], P. Pérez[5], J-M. Rey[5], J-M. Reymond[5], Y. Sacquin[5], B. Vallage[5], O. Dalkarov[6], N. Kolachevskiy[6], K. Khabarova[6], A. Voronin[6], F. Biraben[7], P. Cladé[7], A. Douillet[7], G. Dufour[7], S. Guellati[7], L. Hilico[7], P. Indelicato[7], A. Lambrecht[7], J-P. Karr[7], F. Nez[7], S. Reynaud[7], V-Q. Tran[7], F. Schmidt-Kaler[8], S. Wolf [8], J. Walz[8], M. Staszczak[9], S. Wronka[9], A. Mohri[10], Y. Yamazaki[10], M. Charlton[11], S. Eriksson[11], N. Madsen[11], D.P. van der Werf [11], N. Kuroda[12], Y. Matsuda[12], H. Torii[12], Y. Nagashima[13], P. Froelich[14], S. Jonsell[15]

1. CSNSM Orsay (FR), 2. ETH Zurich (CH), 3. ILL Grenoble (FR), 4. IPCMS Strasbourg (FR), 5. IRFU Saclay (FR), 6. Lebedev Moscow (RU), 7. LKB Paris, (FR), 8. JGU Mainz (GE), 9. NCBJ Otwock-Swierk (PL), 10. RIKEN (JP), 11. Swansea University (UK), 12. University of Tokyo, Komaba, (JP), 13. Tokyo University of Science, (JP), 14. Uppsala University (SE), 15. Stockholm University (SE).

CERN-SPSC-2014-011 / SPSC-SR-136
24/03/2014

1- Introduction

The GBAR experiment is broadly divided into four sections: antiproton deceleration and focussing, positron production and accumulation, antihydrogen cooling and preparation, and detection. A schematic view illustrating this functional breakdown is shown in Figure 1.

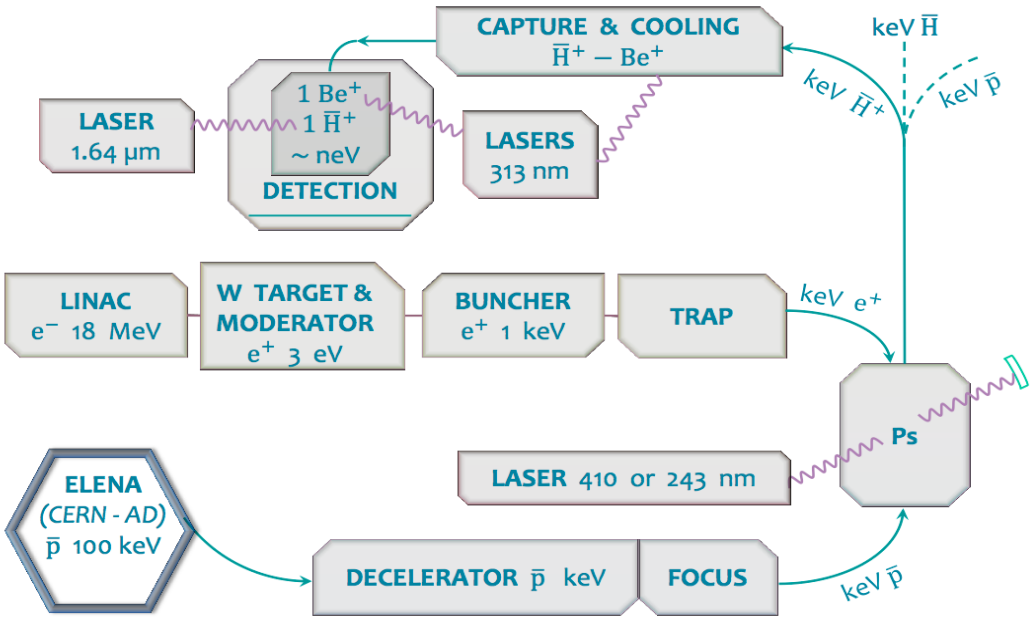

Figure 1 *- Schematic illustration of the GBAR experiment. The MeV and keV values are mean kinetic energies, while the eV and neV values are dispersions, i.e. temperatures, or quantum levels.*

2- Layout

A preliminary layout of the GBAR experiment in the AD Hall is shown in Figure 2.

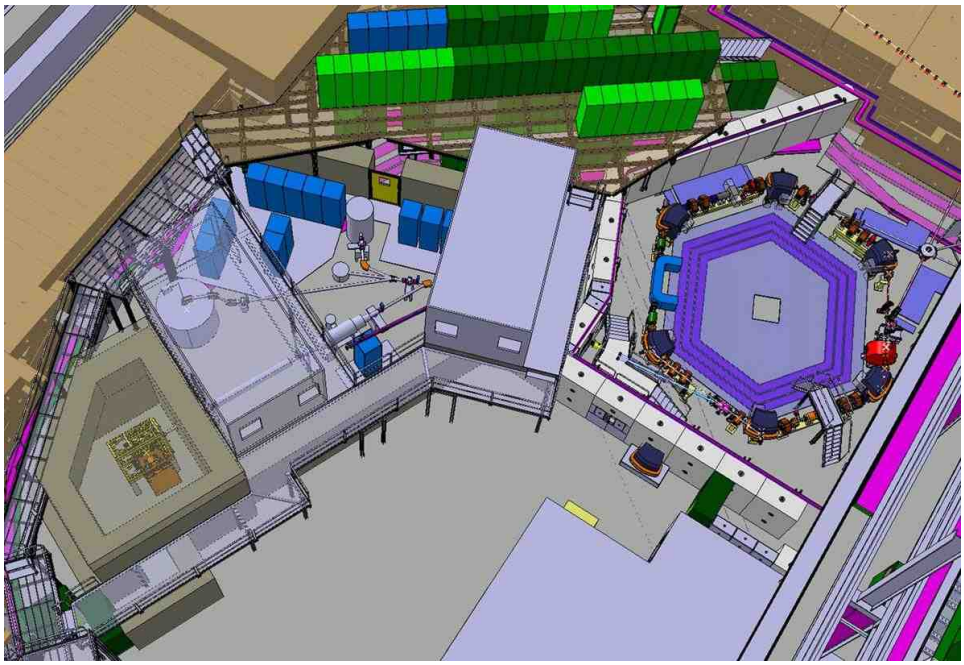

Figure 2 *– Present view of the future layout of the experiment in the CERN AD hall.*

The ELENA beam exits the ring to the left and is transported through two quadrupole doublets to GBAR. The low-energy antiprotons are then deflected left into the reaction chamber. The linac, shown on the lower left (surrounded by shielding) is used to create positrons that are sent to the Penning trap (center) and the accumulated pulse is deflected to the right, into the reaction chamber to form the positronium cloud. The cylinder on the left houses both the antihydrogen capture and cooling traps. The detector is located underneath. Also visible are two mezzanines that will house the laser systems for positronium excitation (right) and cooling and photo-detachment (left). The linac is oriented at 45 degrees with respect to the vertical in order to minimize the height of the bunker and to direct the major part of radiation to the ground. The concrete walls are 80 cm thick. However, if the energy of the linac were increased to 18-20 MeV (see section 4), a preliminary calculation [FRO14] shows that 160 cm is required and should be made of alternating layers of concrete and iron in order to maintain the zone outside the bunker as "public area". Moreover, activation of the materials surrounding the linac would require serious safety procedures and prevent frequent opening of the bunker.

3- Development of the antiproton decelerator in Orsay

The antiproton pulse-down decelerator development continues in Orsay. Using the low-energy (10 keV) test bench facility, we have successfully decelerated large pulses of 5 keV N_2^+ ions down to a few hundred eV. A beam collimator to produce something close to the expected emittance of the ELENA beam has reduced the large emittance. Ion currents in excess of 10 μA have been obtained which we have chopped to 100 ns, producing pulses of about 10^7 ions – very similar to the projected ELENA intensity. A schematic illustration and photograph are shown in Figure 3. A rough characterisation of the decelerated pulses has been achieved and is very close to that expected from simulations.

We are in the process of upgrading the high-voltage cage to 100 kV and we expect to achieve this during the summer of 2014. In parallel, we are preparing for the installation of the 100 keV fast switches (however the delivery of the switches has been delayed by several months; a frequent occurrence given that the company - Behlke - has a monopoly of these devices). We have refined the decelerator electrostatic optics configuration, now incorporating a two-step deceleration process, using modular triplets of cylindrical lenses (Figure 3). These electrodes will be fabricated in the next 2-3 months. We are in discussion with the ELENA group (Roberto Kersevan) for defining the UHV and a-magnetic components for the decelerator chambers. These will be ordered in the upcoming weeks to complement or replace the present parts.

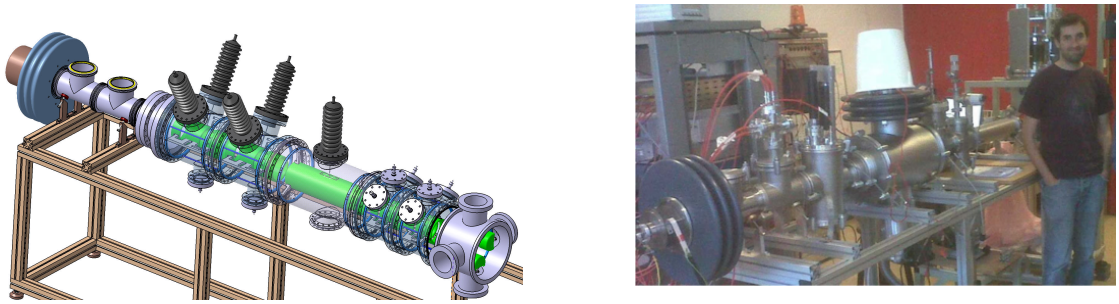

Figure 3 *– (left) schematic and (right) photograph of the decelerator test bench in Orsay.*

At the recent ADUC meeting (January 2014) we presented beam optics calculations that were performed taking into account the beam transfer matrix provided by the ELENA group. While the large ELENA energy spread still adversely affects the transmission (causing losses of over 50%) the entire range of phase space orientation (beam spot size and divergence) from the ELENA transfer line optics can be accommodated by the decelerator electrostatic optics. This means that we expect no difficulties in beam optics at the so-called handover point from ELENA to GBAR. About 30 % transmission is possible through a 20-mm long, 1-mm diameter chamber using electrostatic quadrupoles or cylindrical Einzel lenses for focusing.

The $\overline{H}^+$ ions produced after interaction of the antiprotons with the Ps target located in this small chamber must further be caught in an electrostatic trap (see section 9). The capture in this trap is only efficient if the incoming ion energy spread is lower than 20 eV. However, the expected spread is about 10 times higher from the above simulations. It is thus necessary to find a cooling scheme. An electrostatic ion beam trap (EIBT), available from the team at the LKB laboratory, is being tested at CSNSM Orsay, presently with K^+ ions. The idea is to trap antiprotons and to decrease their energy spread using resistive cooling or stochastic cooling [EIBT]. We may expect 30% efficiency for such cooling to match the capture trap criteria.

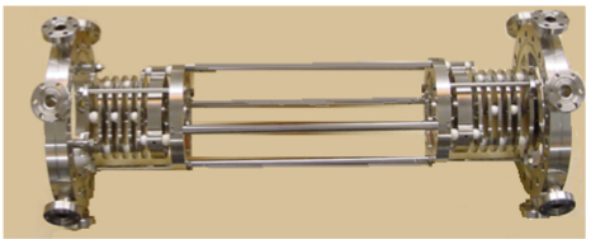

Figure 4 *– EIBT trap from LKB Paris laboratory now at CSNSM Orsay.*

This work is financed by the French P2IO LabEx (ANR-10-LABX-0038) in the framework "Investissements d'Avenir" (ANR-11-IDEX-0003-01) managed by the French National Research Agency (ANR).

4- Linac design

The positron flux needed for the experiment requires an optimisation of the energy/intensity of the electron linac to produce MeV positrons and of the moderation efficiency to obtain the slow positrons that can be accumulated in the Penning-Malmberg trap: the fast positron intensity increases with electron energy and current while the moderation efficiency decreases when the fast positron energy increases. We are presently using a tungsten mesh moderator in our test setup in Saclay with a 4.3 MeV / 0.07 mA (average current) linac resulting in 3×10^6 slow e^+/s. We have estimated, based on a GEANT simulation, that the slow positron flux increases linearly with electron energy in this range. With our measured flux in Saclay and those quoted in the literature, we estimate that we can reach a slow positron flux of 1×10^8 slow e^+/s with a 9 MeV machine running at 300 Hz and 2 µs pulses of 330 mA peak current, i.e. 0.2 mA average current. In order to gain a factor 3 to 4, we would need to increase the electron energy by a factor 2.

The NCBJ group proposes to build a standing wave setup composed of two "9 MeV type" accelerating structures driven by two 7 MW klystrons. Each set of structures comprises 18 RF cavities (see Figure 4). The NCBJ institute has experience in building such 9 MeV linacs using widely available parts such as a triode gun, the 3 GHz TH2157a klystrons running at 10 kW average power and Scandinova solid-state modulators while the RF cavity structures are made, assembled, brazed and tuned in the institute (Figure 5). The RF windows in such a system are less stressed than when a single high power klystron is coupled to a single accelerating structure. The repetition rate is 300 Hz with 300 mA peak current within pulses of length adjustable between 2 to 4 µs, i.e. average current of 0.18 to 0.36 mA. The total length of the accelerating tube is 1.75 m.

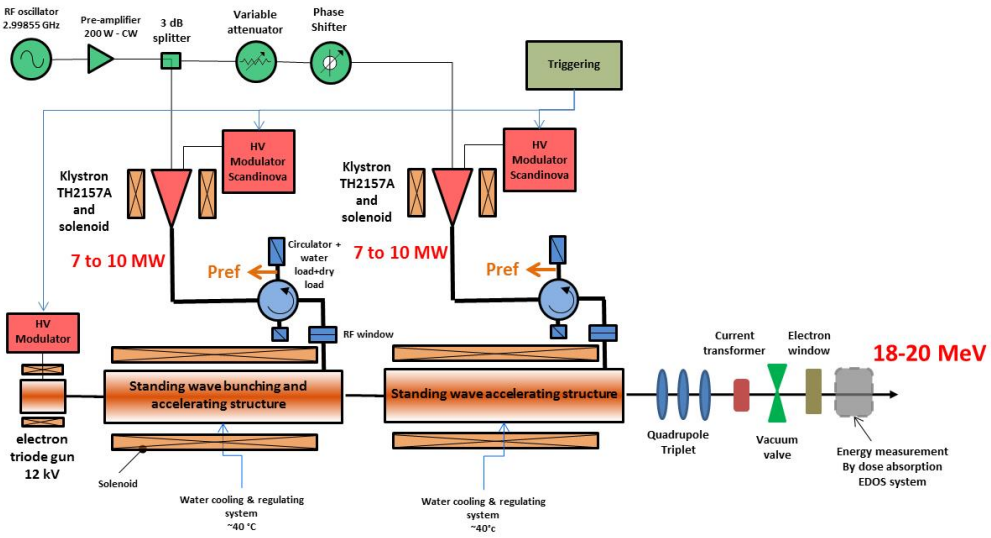

Figure 5 *– Functional diagram of electron linac.*

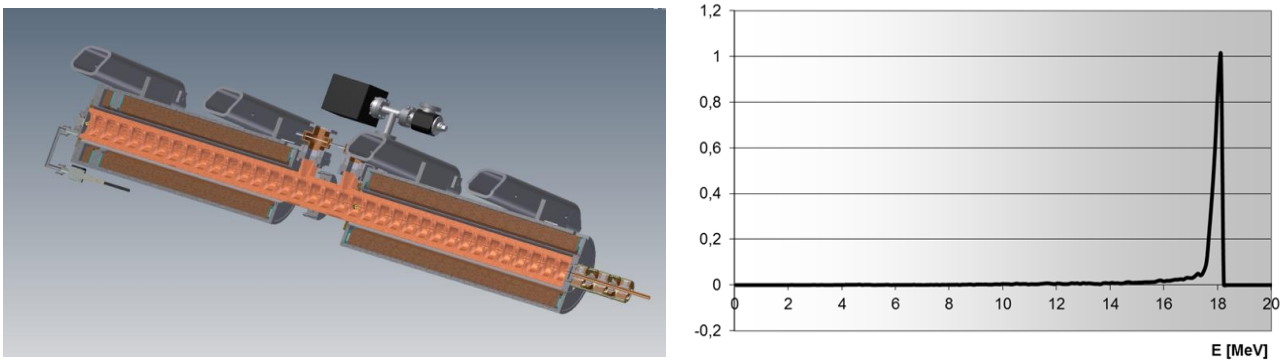

***Figure 6** – CAD view of the two RF cavity linac setup (left) and energy distribution of the electron beam (right).*

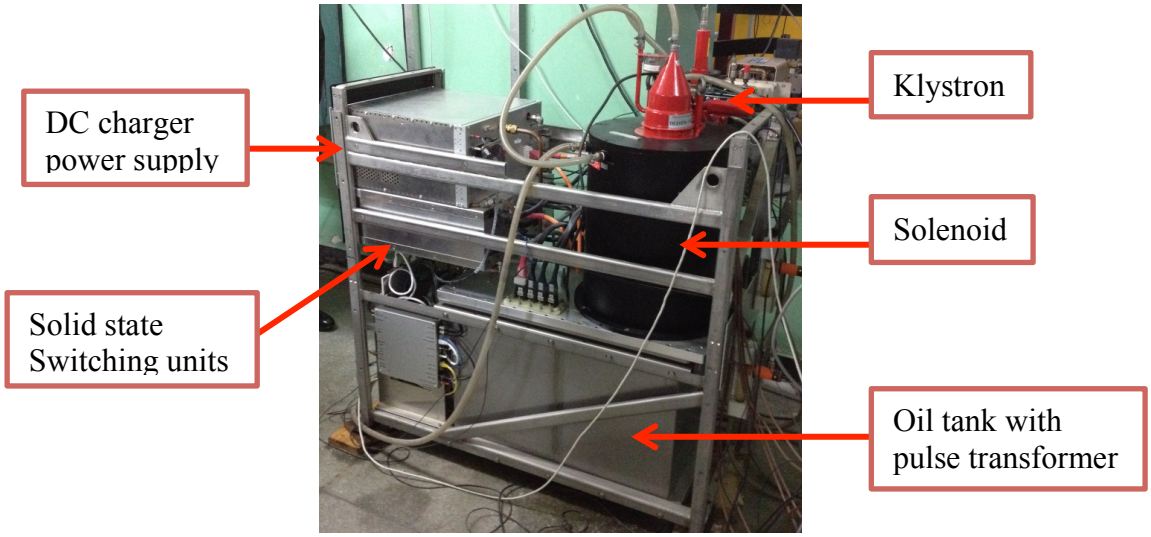

***Figure 7** – Example of a Scandinova modulator and TH2175 Thales klystron with its focusing solenoid.*

The proposed bi-structure allows flexibility both technically and financially. A first setup with half the accelerating structures and corresponding klystron/modulator would allow starting the experiment already in excellent conditions. Discussions are underway to find funding for the parts that must be acquired. The planning possibilities at NCBJ result in a construction duration of 17 months for the bi-structure linac.

5- Demonstrator of positron production and accumulation in Saclay

The 4.3 MeV electron linac at Saclay, equipped with a tungsten target and moderator mesh, produces 3×10^6 slow e^+/s. The positrons are transported to a switch where they can be directed either towards a Penning-Malmberg trap or towards a positron annihilation spectrometer (see previous report and below). The trapping mechanism is depicted in figure 8. The slow positron bunches enter the trapping area and are reflected by a potential barrier at the downstream end of the trap. Before the positrons exit the trap (round trip in 80 ns) the potential of the first upstream electrode is raised in order to block them inside. These slow positrons are cooled by a preloaded electron plasma of 10^{11} cm^{-3} density. The cooling time is expected to be less than the

3 ms between two bunches. The cooled positrons are stored in a second potential well of opposite polarity [DUP13].

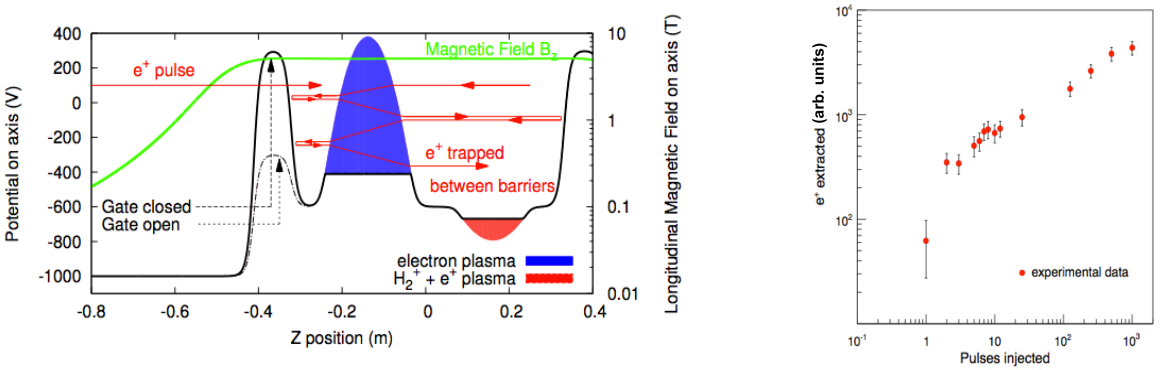

***Figure 8** – Scheme of trapping voltages with e^- cooling (left) and e^+ stacking as a function of pulse number (right).*

First attempts at accumulating positrons were performed in spite of degraded conditions due to several hardware failures. Plasmas of 3×10^{10} electrons of densities 10^{11} cm^{-3} were obtained with lifetimes greater than 500 s, i.e. already sufficient for GBAR. It was shown that accumulation occurred when the electron plasma was present (Figure 8). Positron plasmas of 40 s lifetime were obtained [GRAN13]. Injection and trapping efficiencies must now be largely improved to match the requirements of the experiment.

We constructed and tested an ortho-positronium spectrometer that is implemented on the second beam line. More than 10^5 e^+/s are incident on the sample, depending on the required beam diameter. The spectrometer uses secondary electrons, ejected by the impinging positrons, as start signal (detected by a micro-channel plate detector) and one of the annihilation gamma photons as stop signal. Two large (55 mm diameter, 200 mm long) BGO (bismuth germanate) scintillation detectors are used for gamma detection with large acceptance. The lifetime spectrometer makes use of the quasi-continuous slow positron beam provided by the positron pulse stretcher, with a collimator of variable diameter to limit the beam diameter on the sample. The positron energy (1-8 keV) is set by applying a high voltage on the sample holder.

The lifetime spectrometer has been successfully commissioned and is in use. It has been tested using samples previously measured in other laboratories. We found good agreement with the previous results (Figure 9) [LISZ13]. We started studies of various positron-positronium converter films and are working on the development of some key components for the GBAR installation (remoderator, target cavity).

This work is financed by IRFU and by the French ANR project POSITRAP (ANR 2010 BLAN 0420 02).

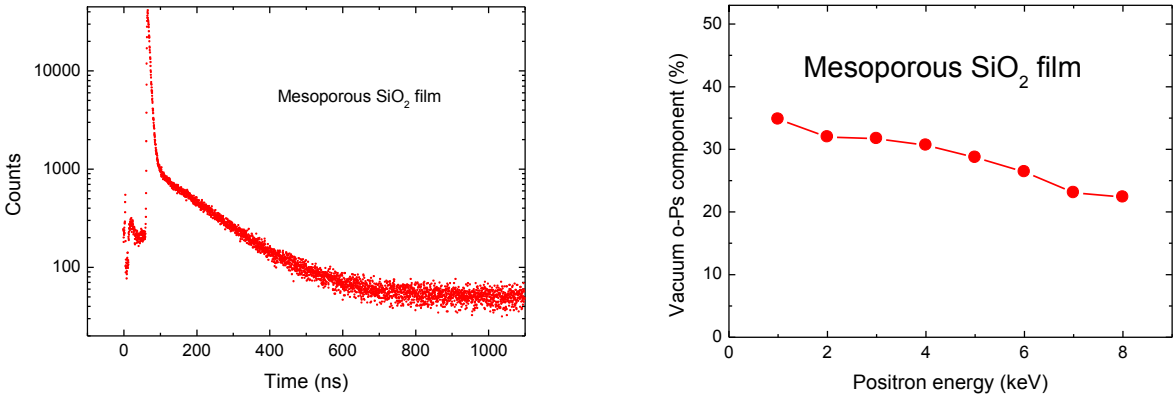

Figure 9 *– Positron lifetime at 3 keV positron energy in a mesoporous silica film deposited on silicon (left) and intensity of the vacuum (142 ns) ortho-positronium component as a function of the positron beam energy (right).*

6- $\overline{H}^+$ production estimates

The production cross sections of $\overline{H}^+$ ions calculated in [COM13] are used to estimate the number of ions that can be produced in GBAR. Since the ion is only efficiently produced with antihydrogen in the ground state interacting with Ps, the reaction chamber tube cell should be several cm long. The timing of the antiproton, positron, and Ps excitation laser illumination pulses are optimised. For a 2 cm long reaction tube, the number of produced ions is of order 1 per ELENA pulse, i.e. 3 times more than in the GBAR proposal [COM14].

7- Reaction region

The interaction of antiprotons with the target positronium cloud will take place inside a tube of 1 mm^2 cross section (see Figure 10). The walls of this tube are made of Silicium coated with nanoporous SiO_2 on the inside. The positron bunch extracted from the trap interacts with these walls to form Ps, itself excited by laser beams. The $\overline{H}$ and $\overline{H}^+$ are created with basically the same energy as the incoming antiprotons. As mentioned in section 3 a major problem is to focus the antiproton beam onto this tube. A similar problem arises for the positrons. They must be ejected from the high field (5 T) Penning-Malmberg trap toward this tube where no magnetic field is present. A first step toward solving this problem was experimented at ETHZ using their slow positron beam as a preparation for Ps 1S-2S-spectroscopy experiment. A target tube was made with coating on one side with the same SiO_2 layer as envisaged for GBAR and on the other side equipped with a 30 nm thick entrance window made of SiN. It was shown that transmission at 5 keV is close to 100%. The Ps formation efficiency is consistent with measurements performed when the incoming e^+ beam interacts directly with the SiO_2 layer and the same Ps lifetime distribution is measured [CRI13].

In order to manage the transport of the positrons from the Penning-Malmberg trap toward the reaction tube their energy distribution must be small. If the positron beam is made to interact on a surface such as tungsten single crystal, the out coming beam energy spread is reduced to 0.1 eV at the expense of an efficiency of the order of 10% for energies in the keV range. When Tungsten is replaced by solid Neon, the efficiency may reach 70% with an energy spread quite acceptable of 1 eV. Such re-moderators have been used in reflection mode in order to keep a high efficiency. The arrangement shown in Figure 11 allows realising such re-moderation in

the same vacuum transport tube (half tube in green in the picture obtained with a CAD software). Simulations show that the transport efficiency is close to 100%. An experimental test will be performed on the beam at Saclay.

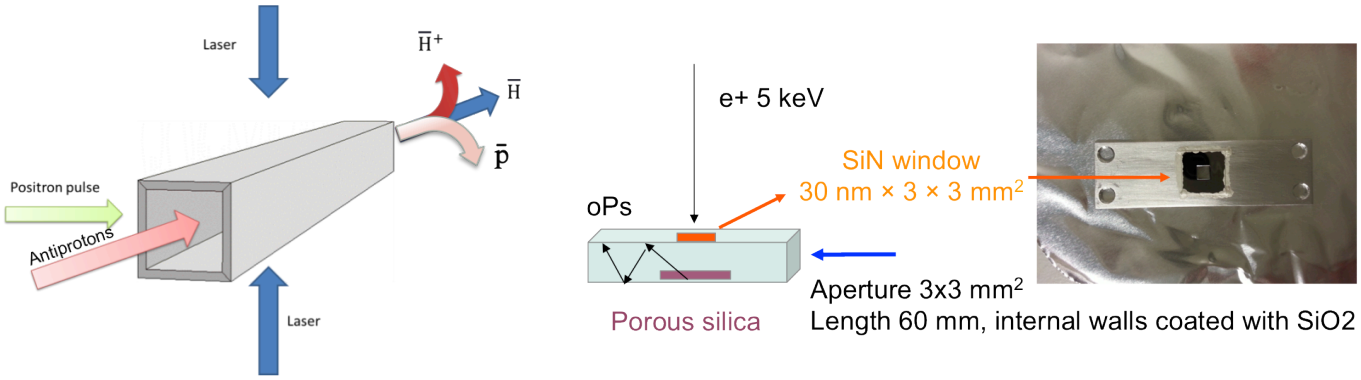

Figure 10 *– Sketch of interaction region (left) and SiN window test (right).*

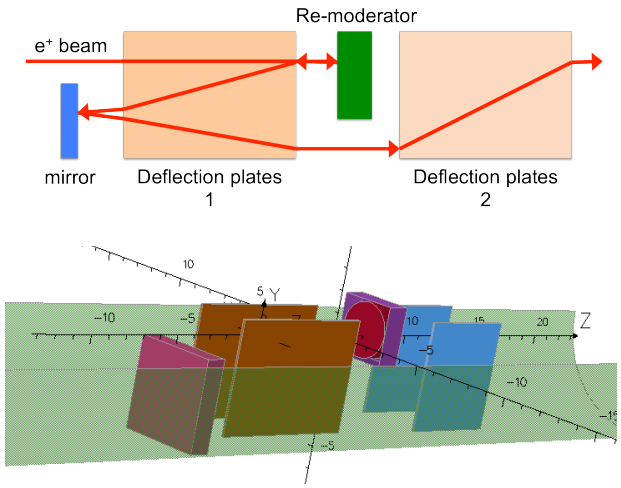

Figure 11 *– Sketch of re-moderator (top) and CAD view (bottom).*

8- Ps excitation

The laser system is prepared at LKB to excite the Ps 3D level (Figure 12). The laser system is made of a cw TiSa that seeds a pulsed TiSa. Presently the cw TiSa is realized and the pulsed TiSa is delivering more than the requirements of the proposal (energy of 4 mJ at 799 nm, 10 ns pulse duration for 20 mJ of 532 nm pump laser). This has to be confirmed at the Ps excitation wavelength (820 nm), although no large changes are expected. The next step is the measurement of the frequency chirp of the pulsed laser by different means.
A study of the two-photon spectroscopy at 820 nm of the 6S-8S transition of Cs will be performed soon in order to test the laser system on a well-known transition but also to test a

detection scheme foreseen for experiments at Saclay. The geometry of the Cs cell, filled at LKB, reproduces the geometry of these experiments.
A TiSa amplifier is also being built to reach around 10 mJ at 410 nm in order to be able to excite a 3 mm diameter Ps beam at Saclay for example. The LBO crystal in which the frequency doubling will occur has been ordered.
A laser hut is being installed at Saclay to experiment on the Ps to be produced at the positron trap exit.

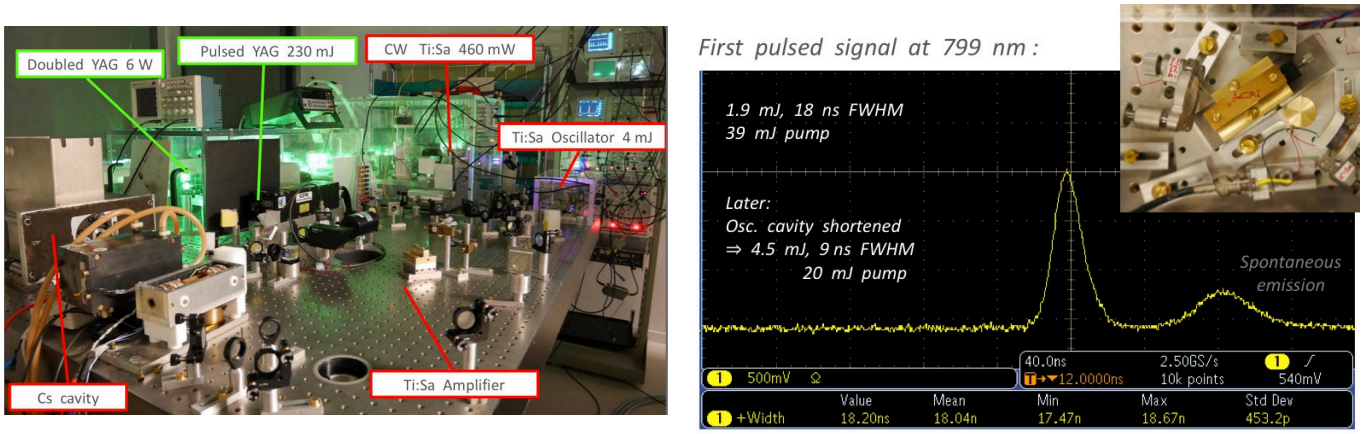

Figure 12 – Optics table for Ps excitation laser *(left) and pulsed 799 nm signal (right).*

9- $\overline{H}^+$ capture and cooling

The schemes studied for $\overline{H}^+$ cooling are described in detail in the proceeding of the last WAG conference [HIL14]. We will use capture and Doppler laser cooling in a mm scale RF linear trap before transferring a single $\overline{H}^+$ ion into a miniaturized trap (called precision trap in the following) to perform ground state cooling of a $Be^+/\ \overline{H}^+$ ion pair. The capture apparatus is made of an RF quadrupole guide and a biased segmented linear trap. Detailed simulations of the capture and cooling processes have been performed. The capture efficiency depends on the kinetic energy spread ΔE of the injected $\overline{H}^+$ ions, being greater than 50% for $\Delta E < 20$ eV thus requiring treatment upstream and downstream of the production point. Motional coupling between ions of different masses decreases with their mass ratio. It is therefore interesting to use an intermediate mass ion compared to $^9Be^+$ such as HD^+. A mixture of 10% HD^+ and 90% Be^+ allows cooling times in the ms range for $\overline{H}^+$ (Figure 13). Then the $\overline{H}^+$ ion is injected in the precision trap to form a $Be^+/\ \overline{H}^+$ ion pair on which ground state Raman side band cooling can be performed. The precision trap consists of four gold coated, micro-fabricated alumina chips that are arranged in an x-shaped configuration and two end caps made from Titanium. The end caps are pierced with a hole with a diameter of 600 µm to enable ion injection into the trap. Two of the chips provide the RF-field and two the DC trapping potential respectively. The corresponding ground state kinetic energies are 0.09 and 0.41 mK for Be^+ and $\overline{H}^+$. Raman sideband sympathetic cooling down to the vibrational ground state of the trap is feasible in less than one second, preparing an $\overline{H}^+$ ion with a velocity dispersion of about 1 m/s.

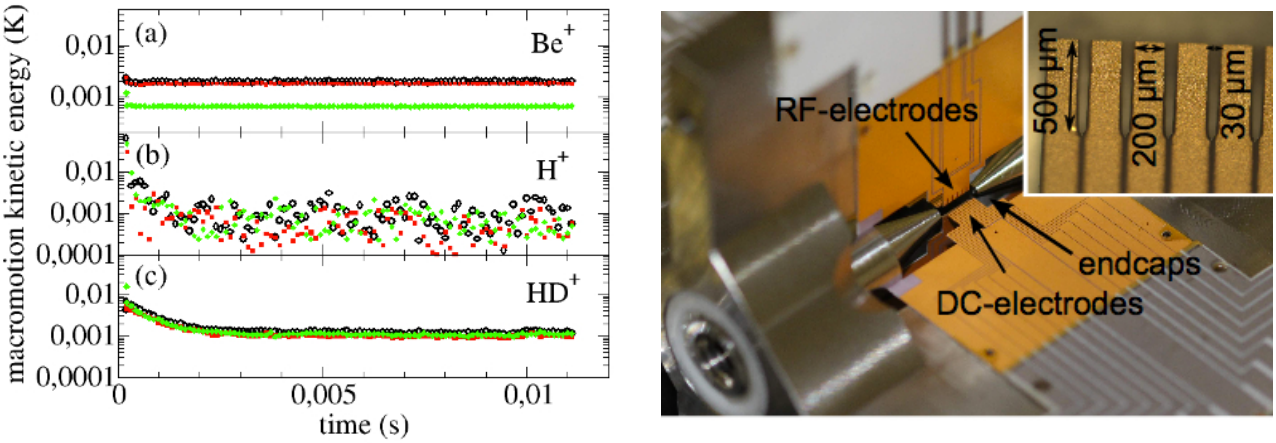

Figure 13 – Sympathetic cooling dynamics of 1800 Be^+/200 HD^+/1 $\bar{H}^+$ mixed ion cloud *(left) and precision trap (right).*

A joint ANR and DFG grant BESCOOL ANR 13-ISO4-0002 was obtained in 2013 by the Paris and Mainz groups to develop a universal setup for transport, capture, and cooling of ions produced outside of the Paul trap. Indeed, the antihydrogen ions will have to be transported from the reaction region to the Paul trap as opposed to ordinary matter ions that are usually produced in situ within the trap by electron impact or photo-ionisation. The same grant will allow to experimentally investigate sympathetic cooling dynamics in the regime of high q/m differences, such as for the couple Be^+/ $\bar{H}^+$, and to develop cooling methods and trap geometries specifically adapted to this case. The objective is to deliver the complete setup for $\bar{H}^+$ capture and cooling, tested with $\bar{H}^+$ ions before final assembly in 2017 at CERN. The first part of the 313 nm Be^+ cooling laser, a 2 W 626 nm source is achieved. The second harmonic generation is being prepared. Tests using Ca^+/Be^+ and Sr^+/Be^+ with mass ratios of 40/9 and 86/9 will be performed within 1.5 to 2 years from now at Mainz and Paris (Figure 14).

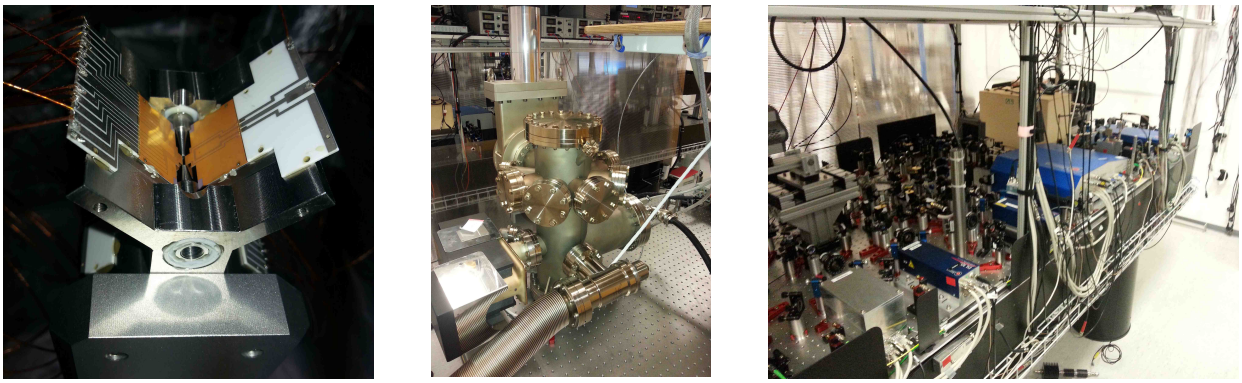

Figure 14 – *Precision trap (left), vacuum setup (middle) and optics table (right) in Mainz.*

10- Detection

The precision of the measurement of $\bar{g}$ depends crucially on the dispersion of initial vertical velocities of the atoms as well as on the reliable control of their distribution. We will use a new method for shaping the distribution of the vertical velocities of $\bar{H}$, which improves these factors simultaneously [DUF14]. The distribution of initial vertical velocities is shaped by selecting the atoms passing through a device consisting of two disks mounted around the

precision trap. The large loss of statistics is more than compensated by the reduction in the spread of the time distribution (Figure 15).

Monte-Carlo simulations indicate that a set of two absorber rings with a minimum radius of 1 mm and a maximum radius of 7 mm separated by 50 microns are optimal for a free fall height of 10 cm. Keeping as a goal a 1% uncertainty on $\bar{g}$, the number of antihydrogen atoms produced is reduced by a factor 10 with a detector radius of 25 cm. Further simulations are underway to take into account losses that will occur for instance in the Paul trap.

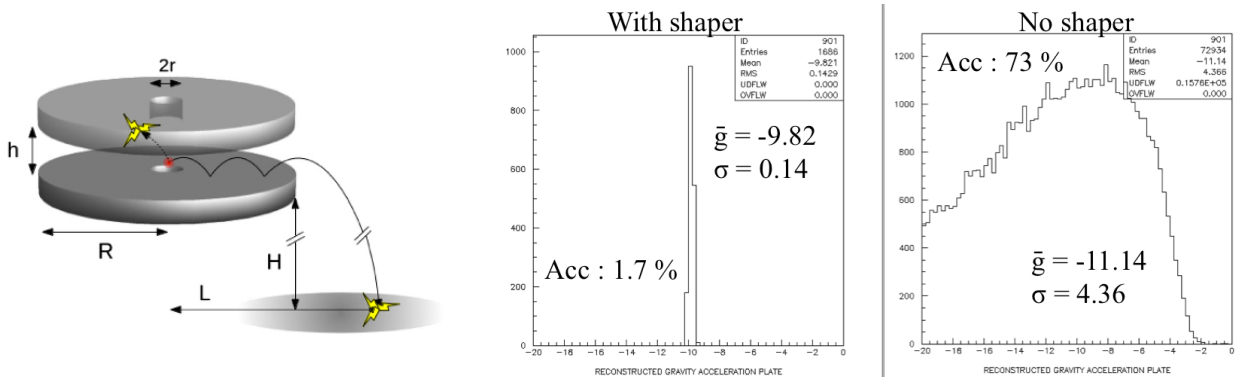

***Figure 15** – Scheme of principle of the shaping device (left) and expected reconstructed $\bar{g}$ distributions with and without shaper (right).*

Detection of the $\bar{p}$-p annihilation will be based on the detection of the charged pions emitted with a few hundred MeV from the annihilation vertex. In the simplest scheme envisaged, the vacuum vessel containing the Paul trap will be a stainless steel cylinder of diameter of the order of 50 cm, and the annihilation plate will be the almost flat bottom of the vessel. The detection requires both vertex position reconstruction, provided by a charged particle tracker, and accurate timing of the annihilation, using a set of scintillating counters surrounding the tracker.

Tracking will consist of a set of planar chambers allowing for the measurement of both X and Y coordinates with an accuracy of a few hundred microns. The newly developed resistive XY MicroMegas detectors of dimensions 50 × 50 cm^2 with a pitch of the order of 500 microns provide such precision with good efficiency, for a chamber total depth of 1 cm. In order to ensure an overall good tracking efficiency, each of the 5 faces surrounding the vacuum vessel (bottom and 4 sides) will be equipped with 3 layers of chambers, for a total lever arm of 10 cm for tracks normal to the chambers. This configuration will result in a spatial resolution of the order of 1 mm at the vertex extrapolated to the annihilation plate. Each view will comprise about 1024 strips spaced every 500 microns (Figure 16). Since most of the activity detected in the chambers will be coming from cosmic background with typical rates of 150 Hz/m^2, a great reduction of electronic channels and subsequent costs will be obtained with the use of "genetic multiplexing" [PROC13]. In such a scheme, an entire plane of 1024 strips can be readout by 64 electronic channels, corresponding to a single chip of the family developed for MicroMegas TPCs and trackers (AFTER, AGET, DREAM,…). Current front-end boards developed for instance for GET, MINOS, CLAS12 and ASACUSA, house 8 such 64 channels chips. The design with 15 bi-dimensional detection chambers will then only require 4 front-end boards, connected to the detectors by low-capacitance micro-coaxial cables.

Scintillating counters will surround the MicroMegas tracker in a hermetic way, meaning that the upper part of the vacuum vessel will be covered as much as possible. Standard scintillating plates will be used, read out by standard photo multipliers (no magnetic field in the detection region) whose signals will be used to form the trigger decision transmitted to the tracker readout system.

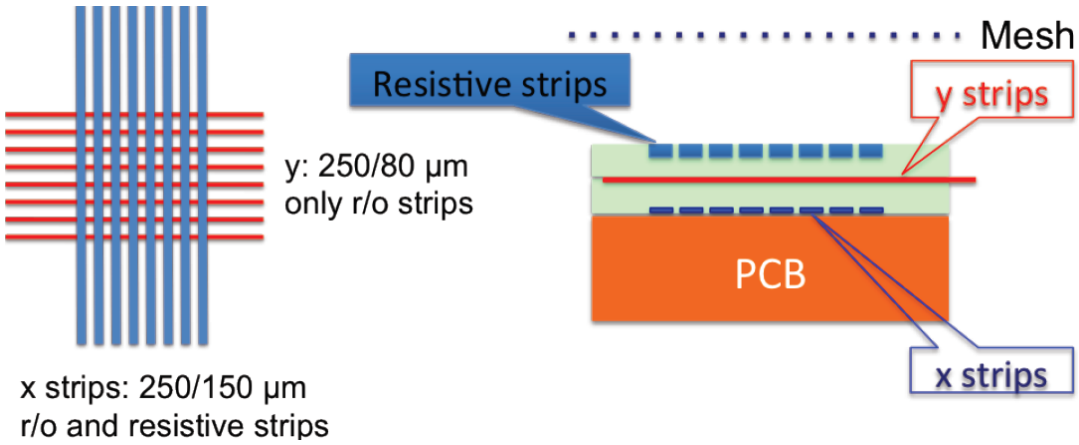

Figure 16 *– Sketch of MicroMegas detector design.*

11- Conclusion

The collaboration groups are actively investigating the elements that will form the major parts of the GBAR experiment as described in the previous sections. These efforts will be continued as formalised in the memorandum of understanding that was finalised on February 9, 2014 and signed by the Director of Research. Today already 8 out the 17 funding agencies for GBAR have sent their signed copy back to CERN.

References

[COM13] P. Comini and P-A. Hervieux, *$\overline{H}$ and $\overline{H}^+$ production cross-sections for the GBAR experiment*, J. Phys.: Conf. Ser. **443**, 012007 (2013).

[COM14] P. Comini, P-A. Hervieux and F. Biraben, *$\overline{H}$ and $\overline{H}^+$ production from collisions between positronium and keV antiprotons for GBAR,* Proceedings of the LEAP 2013 workshop Hyperf. Int., DOI : 10.1007/s10751-014-1030-y.

[CRI13] P. Crivelli, Proceedings of the Workshop on Antimatter and Gravity, 13-15 Nov. 2013, Bern, Switzerland, to appear in Int. J. Mod. Phys. Conf. Ser.

[DUF14] G. Dufour et al., *Shaping the distribution of vertical velocities of antihydrogen in GBAR,* Eur. Phys. J. **C 74** (2014) 2731.

[DUP13] P. Dupré, *A new scheme to accumulate positrons in a Penning-Malmberg trap with a Linac-based positron pulsed source,* 10th International Workshop on Non-Neutral Plasmas, 27-30 August 2012, Greifswald (Germany); AIP Conf. Proc. **1521**, 113–122 (2013).

[EIBT] D. Zajfman et al., *Electrostatic bottle for long-time storage of fast ion beams*, Phys. Rev. **A 55** (1997) 1577; A. Vallette, C.I. Szabo and P. Indelicato, *Stability of ion confinement for a novel mass spectrometer of infinite mass range,* EPL, **103** (2013) 10009; H. B. Pedersen *et al.*, Phys. Rev. A **65**, 042704 (2002).

[FRO14] Preliminary study by R. Froeschl, CERN-DGS-RP-AS.

[GRAN13] P. Grandemange et al., Proceedings of the 13th International Workshop on Slow Positron Beam Techniques and Applications (SLOPOS13), Munich (Germany), 15–20 September 2013; J. Phys. Con. Ser. (2013) accepted.

[HIL14] L. Hilico et al., *Preparing single ultra-cold antihydrogen atoms for the free-fall in GBAR*, arXiv:1402.1695 [physics.atom-ph] (2014).

[LISZ14] L. Liszkay et al., *Present status of the low energy linac-based slow positron beam and positronium spectrometer in Saclay,* Journal of Physics: Conference Series (accepted for publication)

[PROC13] S. Procureur et al, NIM A 729 (2013) 888-894.